Whyman, *J. Chem. Soc. Chem. Commun.* **1994**, 801 (1994).
6. M. J. Hostetler and R. W. Murray, *Curr. Opin. Colloid Interface Sci.* **2**, 42 (1997).
7. R. L. Whetten *et al.*, *Adv. Mater.* **8**, 428 (1996); A. Badia *et al.*, *Chem. Eur. J.* **2**, 359 (1996).
8. M. M. Alvarez *et al.*, *J. Phys. Chem. B* **101**, 3706 (1997); S. Underwood and P. Mulvaney, *Langmuir* **10**, 3427 (1994).
9. S. J. Green, J. J. Stokes, M. J. Hostetler, J. J. Pietron, R. W. Murray, *J. Phys. Chem. B* **101**, 2663 (1997).
10. R. S. Ingram and R. W. Murray, unpublished results.
11. R. S. Ingram *et al.*, *J. Am. Chem. Soc.* **119**, 9279 (1997).
12. F.-R. F. Fan and A. J. Bard, *Science* **277**, 1791 (1997).
13. E. Hartmann, P. Marquardt, J. Ditterich, P. Radojkovic, H. Steinberger, *Appl. Surf. Sci.* **107**, 197 (1996); T. Sato and H. Ahmed, *Appl. Phys. Lett.* **70**, 2759 (1997); L. Guo, E. Leobandung, S. Y. Chou, *Science* **275**, 649 (1997); R. P. Andres *et al.*, *ibid.* **272**, 1323 (1996).
14. M. Amman, R. Wilkins, E. Ben-Jacob, P. D. Maker, R. C. Jaklevic, *Phys. Rev. B* **43**, 1146 (1991); W. Hofstetter and W. Zwerger, *Phys. Rev. Lett.* **78**, 3737 (1997).
15. These MPCs were prepared and separated as described previously [T. G. Schaaff *et al.*, *J. Phys. Chem. B* **101**, 7885 (1997)], with discrete core-sizes specified by core-mass (or equivalent core diameter or approximate number of Au atoms) as 8 kD (1.1 nm, ~38 Au atoms), 14 kD (1.35 nm, ~75), 22 kD (~1.5 nm, ~110), 28 kD (1.65 nm, ~145), and 38 kD (~1.8 nm, ~200), with a saturation monolayer coverage of butanethiolate (C4) or hexanethiolate (C6).
16. AC impedance measurements, in the same solvent, on a monolayer of C4 28-kD MPCs chemically attached to a Au electrode surface reveal a shallow capacitance minimum at −0.2 V, which we take to be the potential of zero charge. The pzc for the unattached C4 clusters should be the same or very similar.
17. M. D. Porter, T. B. Bright, D. L. Allara, C. E. D. Chidsey, *J. Am. Chem. Soc.* **109**, 3559 (1987).
18. The minor peak near 0 V for the 8-kD MPC is thought to be an impurity due to nonuniform C_{CLU} or initial charge.
19. J. D. Roth *et al.*, *J. Am. Chem. Soc.* **114**, 6159 (1992); M. J. Weaver and X. Gao, *J. Phys. Chem.* **97**, 332 (1993).
20. K. J. Taylor, C. L. Pettiette-Hall, O. Cheshnovsky, R. E. Smalley, *J. Chem. Phys.* **96**, 3319, (1992).
21. Q. Li, F. Wudl, C. Thilgen, R. L. Whetten, F. Diederich, *J. Am. Chem. Soc.* **114**, 3994 (1992).
22. T. Suzuki *et al.*, *ibid.* **115**, 11006 (1993).
23. In Eq. 2, F is Faraday constant, A is electrode area, D and C^* are MPC diffusion coefficient and concentration, respectively, Q_{ADS} is charging of any adsorbed MPC, and Q_{DL} is electrode double-layer charging. For the reverse step, $t^{1/2}$ is replaced by θ, that is, $(\tau^{1/2} + (t - \tau)^{1/2} - t^{1/2})$ where τ is the step reversal time [A. J. Bard and L. R. Faulkner, Eds., *Electrochemical Methods: Fundamentals and Applications* (Wiley, New York, 1980), chap. 5].
24. C. P. Collier, R. J. Saykally, J. J. Shiang, S. E. Henrichs, J. R. Heath, *Science* **277**, 1978 (1997).
25. Supported in part by grants from NSF (R.W.M., R.L.W.) and the U.S. Office of Naval Research (R.W.M.).

24 February 1998; accepted 13 May 1998

Giant Electrostriction and Relaxor Ferroelectric Behavior in Electron-Irradiated Poly(vinylidene fluoride-trifluoroethylene) Copolymer

Q. M. Zhang,* Vivek Bharti, X. Zhao

An exceptionally high electrostrictive response (~4 percent) was observed in electron-irradiated poly(vinylidene fluoride-trifluoroethylene) [P(VDF-TrFE)] copolymer. The material exhibits typical relaxor ferroelectric behavior, suggesting that the electron irradiation breaks up the coherent polarization domain (all-trans chains) in normal ferroelectric P(VDF-TrFE) copolymer into nanopolar regions (nanometer-size, all-trans chains interrupted by trans and gauche bonds) that transform the material into a relaxor ferroelectric. The expanding and contracting of these polar regions under external fields, coupled with a large difference in the lattice strain between the polar and nonpolar phases, generate an ultrahigh strain response.

Materials that generate large mechanical actuation induced by external stimuli including electric field, temperature, and stress have attracted a great deal of attention in recent years. The development goals include achieving a large range of motion with high precision and speed, high strain energy density to generate large forces, and a low fatigue rate for a long lifetime and high reliability. Although there are several active materials currently available, there are few that come close to meeting all of these goals. For instance, piezoceramic and magnetostrictive materials, although they have low hysteresis and fast speed, have low strain levels (~0.1%) (*1*, *2*). Shape memory alloys generate high strain and high force but are often associated with large hysteresis and very slow speed (*3*). Ferroelectric polymers, because they are easily processed, cheap, lightweight, and conform to complicated shapes and surfaces, have been studied for nearly three decades for applications in electromechanical devices (*4*, *5*). However, the low strain level (~0.1%) and strain energy density of current ferroelectric polymers have severely limited their usefulness in these applications.

It should be noted that there is an important class of phenomena that has not been exploited in ferroelectric polymers for electromechanical applications: the large lattice strain and large dimensional change associated with phase transformations in these materials. One such example is poly(vinylidene fluoride), PVDF, and its random copolymer with trifluoroethylene, P(VDF-TrFE), which are the best known and most widely used ferroelectric polymers (*4*, *5*). PVDF and its copolymer P(VDF-TrFE) are semicrystalline polymers that have a morphology of crystallites in an amorphous surrounding. With proper sample treatments a ferroelectric phase (β phase, which has an all-trans conformation as shown in Fig. 1) can be induced in these polymers in the crystalline region (*6*). In compositions of P(VDF-TrFE) copolymers that exhibit a ferroelectric-paraelectric (F-P) transition (conversion of all-trans chains to a mixture of trans and gauche bonds), large lattice strains and sample dimensional changes (~10%) have been observed in x-ray diffraction and thermal expansion experiments (*6*–*8*). One drawback of this large strain associated with the transition is the large hysteresis (*6*–*8*).

It is well known that the existence of hysteresis in ferroelectric materials is due to the energy barrier when switching from one polarization direction to another or when transforming from one phase to another. In ferroelectric ceramic materials, the energy barrier can be significantly reduced or eliminated by reduction of the size of coherent polarization regions to a nanometer scale (*9*). In P(VDF-TrFE) copolymers, one possible approach to achieve this result (reduction of the size of all-trans conformation regions) is to introduce defects into the polymer chains. This may be accomplished with high-energy radiation. The influence of high-energy electrons and gamma irradiation on the dielectric and structural prop-

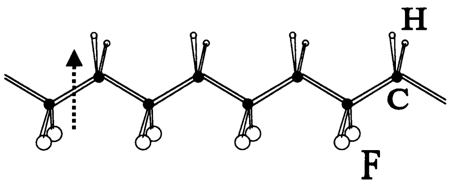

Fig. 1. Schematic depiction of the all-trans chain conformation in PVDF. The arrow indicates the dipole direction.

Materials Research Laboratory and Department of Electrical Engineering, Pennsylvania State University, University Park, PA 16802, USA.

*To whom correspondence should be addressed.

erties of P(VDF-TrFE) copolymers has been studied by several groups (*10–12*). It was found that exposure to these radiations can induce a polymorphic transformation of the ferroelectric phase into a phase that is structurally equivalent to the paraelectric phase. In addition, irradiation shifts the dielectric peak associated with the original F-P transition to a lower temperature and broadens it. These results indicate the effectiveness of the irradiations in changing the dielectric behavior and modifying the structures in these copolymers. Encouraged by these experimental results, we carried out a systematic experimental study of the effect of electron irradiation on ferroelectric and electromechanical responses of P(VDF-TrFE) copolymers, especially under high electric fields.

Here we show that under a proper high-energy electron irradiation the large polarization hysteresis can be eliminated and an exceptionally large electrostrictive strain can be achieved. Furthermore, we present experimental evidence showing that in many respects the material behaves like a relaxor ferroelectric, a class of ferroelectric materials under intensive investigation because of their many peculiar features and broad applications in actuators and transducers, capacitors, and electro-optical devices (*9, 13*).

The results presented here were obtained from P(VDF-TrFE) 50/50 (50 mole percent of VDF), which has a relatively low F-P transition temperature (70°C) and small polarization hysteresis compared with compositions with higher VDF mole percent (*6*). The copolymer was from Solvay and Cie of Bruxelles, Belgium. The film we used was fabricated by melt-pressing powder at 225°C and then slowly cooling it to room temperature. The film thickness was between 25 and 40 μm. The irradiation treatment was carried out in a nitrogen atmosphere with 3-MeV electrons and the dose was in the range between 4×10^5 and 10^6 Gy (1 Gy = 100 rads). Several temperatures were chosen for the irradiation; we report results obtained from films irradiated at 120°C with 4×10^5 Gy. For the electric measurement, gold electrodes sputtered onto the film surfaces were used.

We characterized the electric field–induced strain with a bimorph-based strain sensor designed specifically for polymer film strain measurement (*14*). The polarization hysteresis loop was measured by a Sawyer-Tower circuit (*15*). The frequency range for the polarization and strain measurement was from 1 to 10 Hz. The dielectric constant was evaluated by an HP multifrequency LCR meter equipped with a temperature chamber. The elastic compliance was measured by a dynamic mechanical analyzer in the frequency range from 1 to 200 Hz (*16*). P(VDF-TrFE) 50/50 film measured at room temperature before irradiation exhibited a well-defined ferroelectric polarization hysteresis loop (Fig. 2A) with a coreceive field at 45 MV/m (the field level at $P = 0$ in the hysteresis loop) and a remanent polarization of 6.4 μC/cm² (the polarization level at $E = 0$ in the hysteresis loop). In contrast, the sample irradiated with 4×10^5 Gy at 120°C exhibited a slim hysteresis loop, and the polarization level of the sample was also reduced (Fig. 2B). A similar result was obtained for samples irradiated at room temperature with an electron dose of 8×10^5 Gy. These results show that the defect structure introduced by electron irradiation cannot be recovered by application of high electric fields—which is crucial for electromechanical device applications—whereas the large polarization hysteresis can be removed by irradiation.

After the irradiation, the films showed a high strain response (Fig. 3A). At room temperature, under an electric field of 150 MV/m, which is the limit of the current experiment apparatus, the longitudinal strain (strain in the film thickness direction) can reach more than 4%. In addition, the strain response exhibited little hysteresis and followed an approximately electrostrictive relation between the strain S and polarization P, $S = QP^2$, where the proportional coefficient Q is the charge-related longitudinal electrostrictive coefficient (*17*). As shown in Fig. 3B, the plot of S versus P^2 is nearly a straight line, yielding the electrostrictive coefficient $Q = -13.5$ m⁴/C². In an early study, the electrostrictive coefficient Q of several P(VDF-TrFE) copolymers in the ferroelectric phase was extrapolated from the strain versus polarization hysteresis loop and found to be in the range from –2.1 to –2.5 m⁴/C² (*18*). It should be pointed out that in complex materials like P(VDF-TrFE) copolymers, several polarization mechanisms exist such as those due to the phase transformation, the domain boundary motion, the motion of the interface between crystalline and amorphous phases, and dipolar motion in the polymer chain (*6*). The large increase of Q in the irradiated materials compared with Q in unirradiated ones could be attributed to the difference in the polarization responses in the two materials.

Clearly, materials with such high electrostrictive strain are attractive for actuator, sensor, and transducer applications. However, in very soft polymers the Maxwell stress effect, originating from the coulomb force of the charges, can deform the material to a high strain level (*19, 20*); hence, other parameters such as the strain energy

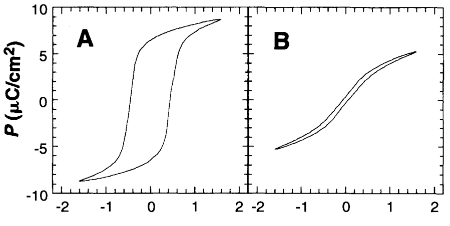

Fig. 2. The polarization hysteresis loops of P(VDF-TrFE) 50/50 copolymer measured at room temperature: (**A**) before irradiation and (**B**) after irradiation with 4×10^5 Gy at 120°C. P is the polarization and E is the electric field.

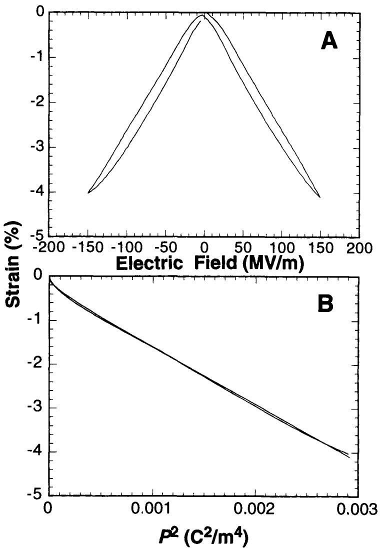

Fig. 3. (**A**) The strain-field dependence of P(VDF-TrFE) 50/50 copolymer after irradiation with 4×10^5 Gy at 120°C. (**B**) The electrostrictive relation between the strain and polarization, where the strains at $P > 0$ and $P < 0$ regions are overlapped as a result of the dependence of P^2 on the strain. The deviation of the data from a straight line at S near zero is due to the zero point uncertainty of the measuring set-up.

Table 1. Comparison of the strain and strain energy density.

Material	Y (GPa)	Typical S_m	$YS_m^2/2$ (J/cm³)	$YS_m^2/2\rho$ (J/kg)
Piezoceramic (*1*)	64	0.1%	0.13	4.25
Magnetostrictor (*2*)	100	0.2%	0.2	21.6
PZN-PT single crystal (*22*)	7.7	1.7%	1.0	131
Polyurethane elastomer (*24*)	0.02	4%	0.016	13
P(VDF-TrFE) electrostrictor	0.38	4%	0.3	160

density are also used to evaluate an actuator material (*21*). In Table 1 we compare the irradiated P(VDF-TrFE) copolymer with several currently known materials, including the ferroelectric relaxor single crystal lead-zinc-niobate/lead-titanate (PZN-PT) and a polyurethane elastomer, which have been shown to have an ultrahigh strain response (*22–24*). Both the volumetric energy density, which is proportional to $YS_m^2/2$ and related to the device volume, and the gravimetric energy density, which is proportional to $YS_m^2/2\rho$ and related to the device weight, are included in the table, where Y is the elastic modulus, S_m is the strain level, and ρ is the density of the material (*21*). Apparently, in terms of the strain and strain energy density, the electrostrictive P(VDF-TrFE) copolymer reported here exhibits a notably improved performance compared with traditional piezoceramic and magnetostrictive materials and is on a par with the PZN-PT single crystal.

To understand what is responsible for the large electrostrictive strain observed in irradiated films, we examined the ferroelectric and dielectric properties. To determine whether P(VDF-TrFE) copolymer after irradiation is a simple dielectric or a ferroelectric, we measured the polarization hysteresis loop at lower temperatures. The polarization hysteresis loop gradually appeared with reduced temperature (Fig. 4); that is, the remanent polarization P_r and coercive field E_c slowly increased with reduced temperature, a feature reminiscent of relaxor ferroelectrics (*9*). In addition, the observed evolution of the polarization response is reproducible under temperature cycles to 120°C, a temperature well above the dielectric peak.

The irradiated film exhibited a broad dielectric peak T_m around room temperature (Fig. 5), which is below the F-P transition temperature (about 70°C) observed in nonirradiated samples. This is consistent with earlier investigations (*11*, *12*). However, unlike the dielectric peak associated with the F-P transition, the data in Fig. 5 show that T_m shifts progressively toward higher temperature with frequency, another feature common to all relaxor ferroelectrics. In addition, as shown in the insert of Fig. 5, the dispersion of T_m with frequency f can be modeled quite well with the Vogel-Folcher (V-F) law

$$f = f_0 \exp[\frac{-U}{k(T_m - T_f)}]$$

a relation observed in many relaxor ferroelectric systems and spin glass systems, where U is a constant related to the activation energy, k is the Boltzmann constant, and T_f can be interpreted as the freezing temperature (*25–27*). The fitting of the data yields f_0 = 9.6 MHz, $U = 6.4 \times 10^{-3}$ eV, and T_f = 307 K (= 34°C).

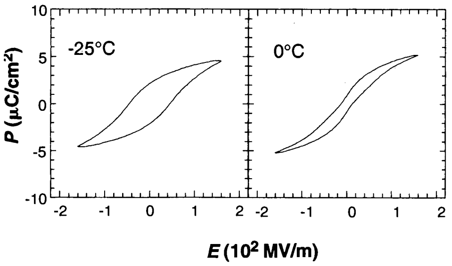

Fig. 4. Polarization hysteresis loops measured at lower temperatures show the gradual increase of the remanent polarization and hysteresis.

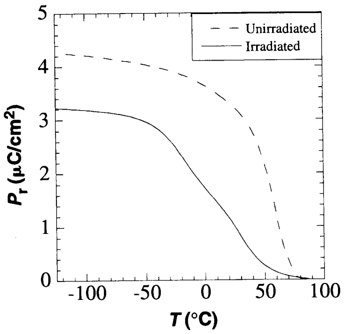

Fig. 6. Remanent polarization P_r as a function of temperature before (dashed line) and after (solid line) irradiation.

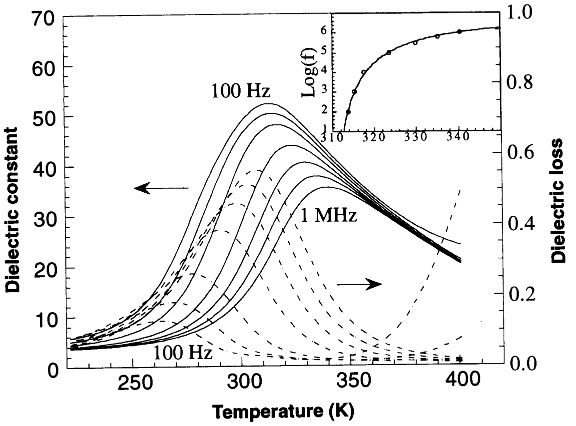

Fig. 5. The dielectric constant (solid lines) and dielectric loss (dashed lines) as a function of temperature for P(VDF-TrFE) 50/50 copolymer after irradiation with 4 × 10^5 Gy at 120°C. The frequency is (from top to bottom curves for dielectric constant and from bottom to top curves for dielectric loss): 100 Hz, 1 kHz, 10 kHz, 100 kHz, 300 kHz, 600 kHz, and 1 MHz. The insert shows the fitting of the Vogel-Folcher law, where the solid line is the fit and the circles are the data [the horizontal axis in the insert is temperature (in kelvin), and f is the frequency].

Before irradiation, a sharp drop of P_r with temperature is seen near 70°C, the F-P transition temperature (Fig. 6), but after irradiation, the change of P_r with temperature is more gradual, typical of ferroelectric relaxors. In addition, the derivative of P_r of the irradiated sample with temperature exhibits two broad peaks, one near –23°C and the other near 32°C. The peak at –23°C is related to the glass transition in the amorphous phase, indicating an increase of the amorphous phase in the irradiated sample compared with the nonirradiated sample (*5*, *6*). The peak near 32°C coincides closely with the freezing temperature determined from the dielectric constant (T_f = 34°C), consistent with the induction by external fields of a macroscopic ferroelectric state in a ferroelectric relaxor below the freezing temperature (*28*).

These results demonstrate that the material after irradiation has many features in common with the relaxor ferroelectric systems in inorganic materials, that is, the slim polarization hysteresis loop at temperatures near the dielectric peak that gradually evolves into a normal ferroelectric polarization hysteresis loop with reduced temperature and the dispersion of the broad dielectric peak, which follows the V-F law. By drawing the analogy with the mesoscopic structure of the relaxor systems in inorganic materials (*9*), the results suggest that the state of the crystalline region of the material after irradiation is not a simple paraelectric but rather a phase containing nanopolar regions (nanometer-size all-trans chains) interrupted by trans and gauche bonds introduced by irradiation. The expanding and contracting of these nanopolar regions under an external field result in the observed slim polarization loop. Because of the large difference in the lattice constant between the polar and nonpolar phases in P(VDF-TrFE) copolymers (*5*, *6*), the gradual increase of polarization with field in the relaxor P(VDF-TrFE) copolymer produces a giant electrostrictive strain with a high strain energy density.

REFERENCES AND NOTES

1. L. E. Cross, *Ceram. Trans.* **68**, 15 (1996); the data in Table 1 is for PZT-4.
2. K. B. Hathaway and A. E. Clark, *Mater. Res. Bull.* **18**, 34 (1993); the data in Table 1 is for terfenol-D.
3. S. M. Wayman, *ibid.*, p. 49.
4. A. J. Lovinger, *Science* **220**, 1115 (1983).
5. K. Tashiro, in *Ferroelectric Polymers*, H. S. Nalwa, Ed. (Dekker, New York, 1995), pp. 63–181.
6. T. Furukawa, *Phase Transition* **18**, 143 (1989).
7. K. Tashiro, K. Takano, M. Kobayashi, Y. Chatani, H. Tadokoro, *Ferroelectrics* **57**, 297 (1984); T. Yamada, T. Ueda, T. Kitayama, *J. Appl. Phys.* **52**, 948 (1981).
8. A. J. Lovinger, D. D. Davis, R. E. Cais, J. M. Kome-

tani, *Polymer* **28**, 617 (1987).
9. L. E. Cross, *Ferroelectrics* **76**, 241 (1987).
10. A. J. Lovinger, *Macromolecules* **18**, 910 (1985).
11. B. Daudin, M. Dubus, J. F. Legrand, *J. Appl. Phys.* **62**, 994 (1987).
12. A. Odajima, Y. Takasa, T. Ishibashi, K. Yuasa, *Jpn. J. Appl. Phys.* **24**, 881 (1985).
13. G. H. Haertling, *Ferroelectrics* **75**, 25 (1987).
14. J. Su, P. Moses, Q. M. Zhang, *Rev. Sci. Instrum*, in press.
15. J. K. Sinha, *ibid.* **42**, 696 (1965).
16. Model DMA 2980, TA Instruments, New Castle, DE.
17. V. Sundar and R. E. Newnham, *Ferroelectrics* **135**, 431 (1992).
18. T. Furukawa and N. Seo, *Jpn. J. Appl. Phys.* **29**, 675 (1990).
19. Q. M. Zhang, J. Su, C. Kim, R. Ting, R. Capps, *J. Appl. Phys.* **81**, 2770 (1997).
20. R. Pelrine, R. D. Kornbluh, J. P. Joseph, *Sens. Actuators* **A64**, 77 (1998).
21. V. Giurgiutiu and C. Rogers, *J. Intell. Mater. Syst. Struct.* **7**, 656 (1996).
22. S.-E. Park and T. Shrout, *J. Appl. Phys.* **82**, 1804 (1997).
23. R. F. Service, *Science* **275**, 1878 (1997).
24. M. Zhenyi, J. I. Scheinbeim, J. W. Lee, B. A. Newman, *J. Polym. Sci. Part B Polym. Phys.* **32**, 2721 (1994).
25. H. Vogel, *Z. Phys.* **22**, 645 (1921); G. S. Fulcher, *J. Am. Ceram. Soc.* **8**, 339 (1925).
26. A. K. Tagantsev, *Phys. Rev. Lett.* **72**, 1100 (1994).
27. J. Mattsson, T. Jonsson, P. Nordblad, H. Aruga, A. Ito, *ibid.* **74**, 4305 (1995).
28. R. Sommer, N. Y. Yushin, J. J. van der Klink, *Phys. Rev. B* **48**, 13230 (1993).
29. We thank L. E. Cross, R. Y. Ting, J. Lindberg, G. Kavarnos, F. Tito, and R. Roy for stimulating discussions. Supported by the Office of Naval Research through grant number N00014-97-1-0900 and NSF through grant number ECS-9710459.

3 February 1998; accepted 23 April 1998

Neptune's Eccentricity and the Nature of the Kuiper Belt

William R. Ward* and Joseph M. Hahn

The small eccentricity of Neptune may be a direct consequence of apsidal wave interaction with the trans-Neptune population of debris called the Kuiper belt. The Kuiper belt is subject to resonant perturbations from Neptune, so that the transport of angular momentum by density waves can result in orbital evolution of Neptune as well as changes in the structure of the Kuiper belt. In particular, for a belt eroded out to the vicinity of Neptune's 2:1 resonance at about 48 astronomical units, Neptune's eccentricity can damp to its current value over the age of the solar system if the belt contains slightly more than an earth mass of material out to about 75 astronomical units.

Beyond the orbit of Neptune lies a recently discovered disk of objects called the Kuiper belt (KB). The first KB object, 1992 QB_1, was found by Jewitt and Luu (*1*). To date, observations have yielded some 55 trans-Neptune bodies like 1992 QB_1 with radii on the order of 100 km or larger. Pluto is considered by some to be a member of this population (*2*). Based on the size of the sky area searched, estimates of the total population of such objects within 10° of the ecliptic is of the order of a few $\times$ 10^4 (*3*). Smaller objects must also be present and the latest survey by Jewitt *et al.* (*4*) puts the total mass between 30 and 50 astronomical units (AU) at earth mass $0.26M_\oplus$ for objects greater than 1 km in diameter. Anderson *et al.* (*5*) have inferred a limit of $\sim 0.3M_\oplus$ out to 65 AU from the lack of penetration of the Pioneer 10's propellant tank by KB debris of radii > 0.5 cm. The discovery of 1996TL_{66} in a high eccentricity orbit points to an additional scattered KB component having a mass of $\sim 0.5M_\oplus$ with orbits between ~40 and 200 AU (*6*).

The dynamics of the KB is also the subject of considerable attention and has led to some indirect estimates of its mass. Residuals in the orbit of Halley's comet have been used to set a mass limit of order of $M_\oplus$ for a ring of comets at ~50 AU (*7*). Duncan *et al.* (*8*) demonstrated that a trans-Neptune disk could provide a plausible source for short-period comets. Test particle simulations appear to require an initial number density profile of $n(r) \sim 3 \times 10^6 \times (40\ \mathrm{AU}/r)^2$ particles per AU^2 to account for the present flux of Jupiter family comets into the inner Solar System. This implies an initial surface density of $\sigma \sim 0.06(R/10\ \mathrm{km})^3$ g/cm^2 and a radial mass gradient $dM/dr \sim 2\pi\sigma r \sim 0.6(R/10\ \mathrm{km})^3\ M_\oplus/\mathrm{AU}$ at $r = 40$ AU. The bulk of these objects are probably comet sized with R equal to a few kilometers.

KB objects (KBOs) are far from uniform in their orbital characteristics, with most objects interior to ~40 AU observed to have high eccentricities and to reside in mean motion resonances with Neptune (9, *10*). These resonant orbits may be instrumental in preserving their occupants; it is well known that Pluto enjoys such protection through its 3:2 resonance that prevents close encounters with Neptune. On the other hand, numerical experiments show that many test particles achieve Neptune crossing status within 10^9 years because of the action of secular and mean motion resonances (9). Thus, the observed inner portion of the belt appears to be highly evolved, and, perhaps, substantially depleted from its primordial density. Extrapolating models of the planetesimal disk into this region implies that a few tens of earth masses originally may have resided there. A substantial disk of a few Neptune masses is required by the resonance sweeping hypothesis (*10, 11*) in which the giant planets migrate, thereby trapping KBOs in low-order mean motion resonances. A massive primordial KB has also been postulated by Stern (*2*), who prefers ~10 to $50M_\oplus$ of material between 30 and 50 AU to collisionally assemble QB_1-type KBOs before Neptune's formation.

Here we introduce another constraint on the nature of the KB that has not yet been exploited. Galactic disks and planetary rings can transport angular momentum by spiral density waves, a process that can alter the orbital evolution of a perturbing body and change the structure of the disk (*12*). For example, many gaps and ringlets of Saturn's rings are due to perturbations from the planet's satellites (*13*), and simulations of planet-forming circumstellar gas disks indicate that density waves may result in the orbital decay of embedded protoplanets (*14, 15*), which, in turn, may have relevance to the existence of close stellar companions (*16*). Neptune's eccentricity is curiously low ($e = 0.009$, where $e = 0$ for a circular orbit) compared with the other planets in the solar system.

Waves are excited at resonance sites, which are locations where a forcing frequency matches some natural frequency of the disk. The most numerous examples are mean motion resonances, where the disk's orbital period is commensurate with the perturber's orbital period. A less common situation involves the apse precession period of disk material as the natural frequency and the disk's wave response is referred to as an apsidal wave. These too have been detected in Saturn's rings, where the forcing frequency is the mean motion of Iapetus (*13*). Also included in this class is the secular resonance where the forcing frequency is the slow apsidal precession rate, ν_p, of the perturber (*17, 18*). The resulting wavelengths are much longer than their mean-motion counterparts, and the wave's open spiral structure allows a perturber to gravitationally couple to a wide swath of the

---

W. R. Ward, Jet Propulsion Laboratory, California Institute of Technology, Pasadena, CA 91109 USA.
J. M. Hahn, Lunar and Planetary Institute, 3600 Bay Area Boulevard, Houston, TX 77058 USA.

*Present address: Southwest Research Institute, 1050 Walnut Street, Suite 429, Boulder, CO 80302 USA.